Journal of Molecular Modeling (2021) 27: 5
https://doi.org/10.1007/s00894-020-04645-5

ORIGINAL PAPER

Theoretical and experimental study of guar gum sulfation

Aleksandr S. Kazachenko [1,2] · Feride Akman [3] · Abir Sagaama [4] · Noureddine Issaoui [4] · Yuriy N. Malyar [1,2] · Natalya Yu. Vasilieva [1,2] · Valentina S. Borovkova [1,2]

Received: 14 August 2020 / Accepted: 10 December 2020 / Published online: 2 January 2021

Abstract

The synthesis of guar gum sulfates by a complex of sulfur trioxide with 1,4-dioxane was studied. The influence of temperature, process duration, and the volume of chlorosulfonic acid on the degree of substitution of guar gum sulfates was studied. The sulfation process has been optimized using the Box-Behnken design. It was shown that the optimal conditions for sulfation of guar gum with a complex of sulfur trioxide-1.4-dioxane: temperature 60 °C, duration 2.9 h, and a volume of chlorosulfonic acid of 3.1 ml. Sulfate groups embedding into the structure of guar gum was confirmed by elemental analysis and FTIR. The initial and sulfated guar gum were also characterized by methods: X-ray diffraction, scanning electron microscopy, and gel permeation chromatography. Using X-ray diffraction, it was shown that amorphization of guar gum occurs during sulfation. Using scanning electron microscopy, it was shown that the morphology of guar gum changes in the process of sulfation. Using gel permeation chromatography, it was shown in the process of guar gum sulfation by a complex of sulfur trioxide with 1,4-dioxane, the molecular weight decreases from 600 to 176 kDa. The geometric parameters of all complexes were carried out by using the DFT/B3PW91 method with a 6-31 + G (d,p) basis set. These structures are optimized to predict the important properties of a theme. MEP with contour map has been performed to obtain the electronic properties. Frontier molecular orbital HOMO-LUMO orbital diagram has been obtained for different energy levels and their band gap energies have been computed.

Keywords Guar gum · Sulfation · Structure · DFT · Sulfated guar gum

Introduction

Plant biomass, consisting of lignin, cellulose, and hemicelluloses, is a renewable resource and an important source of valuable chemicals [1]. Plant polysaccharides are widely used as biomedical preparations with antioxidant, prebiotic, antimutagenic, immunomodulatory, mitogenic, hepatoprotective, and lipid-lowering properties [2]. Due to the combination of the unique properties of polysaccharides (water solubility, low toxicity, biodegradability, dispersing properties, and the ability to retain moisture and bind fat), they are widely used in veterinary medicine, medicine, and in the manufacture of food and cosmetic products [3].

Guar gum is galactomannan—plant polysaccharide consisting of β-(1–4)-D-mannose and α-(1–6)-D-galactose [4, 5]. The main sources of galactomannans from gums are *Ceratonia siliqua* (locust bean), *Cyamopsis tetragonoloba* (guar gum), *Caesalpinia spinosa* (tara gum), and *Trigonellafoenum-graecum* L. (fenugreek gum). Among them, only locust bean and guar gums are of considerable industrial and commercial importance [5].

Galactomannans are non-toxic compounds actively used in the production of food, textile, pharmaceuticals, and medicine as food additives, stabilizers, flocculants, thickeners, and gelling agents [6–9]. The pharmacological studies showed that galactomannans and their derivatives exhibit the anticoagulant [10], hepatoprotective, and analgesic properties [11, 12].

Guar gum (GG) is a food grade carbohydrate polymer that is used as a thickener and as a reagent for absorption and hydrogen bonding with mineral and polysaccharide surfaces

✉ Aleksandr S. Kazachenko
leo_lion_leo@mail.ru

[1] Institute of Chemistry and Chemical Technology SB RAS, Federal Research Center "Krasnoyarsk Science Center SB RAS", Akademgorodok, 50/24, Krasnoyarsk, Russia 660036

[2] Siberian Federal University, Svobodny av., 79, Krasnoyarsk, Russia 660041

[3] Vocational School of Technical Sciences, University of Bingöl, 12000 Bingol, Turkey

[4] Laboratory of Quantum and Statistical Physics (LR18ES18), Faculty of Sciences, University of Monastir, 5079 Monastir, Tunisia

[13, 14]. Guar gum consists of a direct chain of mannose units connected to galactopyranose units. GG is used in explosives, food products, cosmetics, and pharmaceuticals, as well as in the mining, paper, and textile industries, mainly as a binder for water [13, 15].

Derivatives of guar gum are widely used in the oil industry [16] corrosion inhibitors [17, 18], viscosity modifiers [16, 19, 20], fracturing fluids [16, 20], and for the preparation of water-in-oil emulsions [20, 21].

One of the promising directions for the modification of guar gum is the preparation of derivatives containing a sulfate group. Embedding of a sulfate group into biopolymer macromolecule increases its biodegradability and dissolution in water [22]. Sulfated derivatives of guar gum may find application in pharmaceuticals as antiviral drugs, antioxidants, and anticoagulants [23–25].

Currently, complexes of sulfur trioxide with various bases, which are used not only to obtain a sulfating mixture but also as a reaction medium, are widely used as sulfating reagents for hydroxyl-containing organic compounds [26].

The synthesis of guar gum sulfates is mainly based on methods in which complexes of sulfur trioxide with toxic amines (in particular pyridine) are used as a sulfating mixture [23–25].

The aim of this work was to optimize the process of guar gum sulfation by a complex of sulfur trioxide with 1,4-dioxane and to study the obtained guar gum sulfates by elemental analysis, IR spectroscopy, X-ray diffraction, scanning electron microscopy, gel permeation chromatography, and DFT. In view of the abovementioned findings and as a continuation of our previous work, we have reported herein the synthesis of new compounds and the structural parameters of new synthesis compounds were obtained by theoretical calculations using the density functional theory (DFT) method with the common B3PW91 function using 6-31 + G (d, p) basis sets.

Experimental

The guar gum (Sigma) was used in the work.

Obtaining a sulfating complex

The complex of 1,4-dioxane and sulfur trioxide, used for sulfation of guar gum, was obtained by the interaction of 1,4-dioxane with chlorosulfonic acid. To do this, 25 ml of dioxane was placed in a three-necked flask equipped with a thermometer, a mechanical stirrer, and a dropping funnel, and with vigorous stirring at a temperature of 20 °C, 1–4 ml (15.2–60.8 mmol) of chlorosulfonic acid was added dropwise.

Sulfation of guar gum

Sulfation of guar gum with a previously obtained complex of sulfur trioxide with 1,4-dioxane was carried out according to the method developed by us. To a complex of sulfur trioxide and 1,4-dioxane, 1.0 g of guar gum was added with stirring at a temperature of 20–40 °C; the reaction mixture was stirred at this temperature for 60–180 min. At the end of the sulfation process, the reaction mass was neutralized with an aqueous solution of sodium hydroxide (or ammonium hydroxide) to a pH of 8 to 9.

Dialysis of sulfated GG

The product was dialyzed against water in a plastic bag of MF-503-46 MFPI brand (USA) with a pore size of 3.5 kDa for 10 h to remove the reactants excess. The water was changed every hour (Fig. 1). In the dialysis process, high molecular weight compounds are purified from low molecular weight impurities (including inorganic compounds). The dissolved high molecular weight part remained in the dialysis bag. The low molecular weight products passed through the membrane of the dialysis bag into the external environment-distilled water.

The degree of substitution (DS) was calculated according [23] to Eq. (1).

$$\mathrm{DS} = \frac{1.62*S\%}{32-1.02*S\%} \quad (1)$$

S% is the sulfur content determination by elemental analysis.

For physico-chemical studies, a sample was taken with a DS of 0.90.

Methods of physico-chemical analysis

Elemental analysis

FlashEA-1112 elemental analyzer (ThermoQuest, Italia) was used for the sulfated guar gum elemental analysis.

Fourier transform infrared spectroscopy

Shimadzu IR Tracer-100 spectrometer (Japan) was used for the obtaining FTIR spectra of initial guar gum and sulfated guar gum within the wavelength range of 400–4000 cm^{-1}. OPUS program (version 5.0) was used for processing the FTIR spectra. Pills in a KBr matrix (2-mg sample/1000 mg KBr) were used for analysis of solid samples.

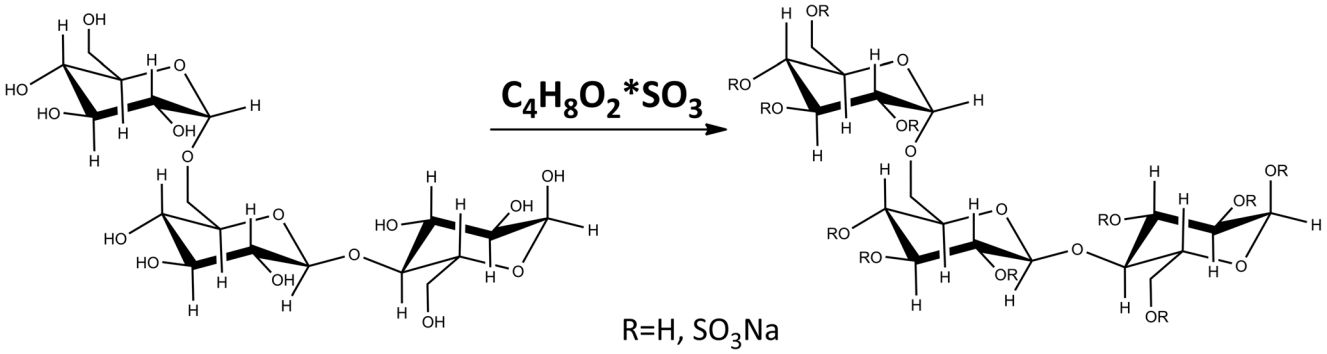

Fig. 1 Scheme of guar gum sulfation reaction with chlorosulfonic acid in 1,4-dioxane

X-ray diffraction

DRON-3 X-ray diffractometer (CuKα monochromatized radiation ($\lambda = 0.154$ nm), voltage 30 kV, current 25 mA) was used for the X-ray diffraction phase analysis. For analysis, the interval of the Bragg angles 2Θ from 5.00 to 70.00 Θ was used.

Scanning electron microscopy

Hitachi TM-1000 scanning electron microscope (Japan) (accelerating voltage of 15 kV and a magnification from × 100 to × 10,000 with a resolution of 30 nm) was used for obtaining electron micrographs. The electron micrographs were processed using the ImageJ software (version 1.8.0_112).

Gel permeation chromatography

Agilent 1260 Infinity II Multi-Detector GPC/SEC System chromatograph (with two detections: refractometer (RI) and viscometer (VS)) was used for obtaining data on the average molecular mass (Mn), average molecular weight (Mw), and polydispersity of the initial and sulfated guar gum. Two Aquagel-OH columns were used for the separation. The solution of 0.2M$NaNO_3$ + 0.01 M NaH_2PO_4 in water (pH = 7) as the mobile phase was used. Calibration was performed using polyethylene glycol standards (Agilent, USA). The flow rate of the eluent was 1 ml/min, with a volume of the used sample—100 μl. Before analysis, the samples were dissolved in the mobile phase (1–5 mg/ml) and filtered through a 0.22-μm PES membrane filter (Agilent). Agilent GPC/SEC MDS software was used for data analysis.

Table 1 Designations of independent variables (factors) and output parameters (experimental results)

Factors and parameters	Notation in equations	Range of variation
Temperature, °C	X_1	*20–60*
Duration of process, h	X_2	*1–3*
Volume CSA, ml	X_3	*1–4*
Degree of substitution	Y_1	–

Numerical optimization of the sulfation guar gum

The software Statgraphics Centurion XVI, DOE block (design of experiment), was used for numerical optimization of the guar gum sulfation process, according to references [27, 28].

Computational details To determine the molecular electronic structure using computer simulation, the theory of the density functional plays an important role. The molecular parameters of all compounds (ground state) were obtained by performing DFT calculations using a functional hybrid B3PW91 with a

Table 2 Effect of guar gum sulfation conditions by chlorosulfonic acid in 1,4-dioxane on the characteristics of the obtained guar gum sulfates

№	Temperature, °C	Duration of process, h	Volume CSA, ml	DS
1	40	2	2.5	0.71
2	60	2	1.0	0.72
3	60	3	2.5	0.90
4	40	3	4.0	0.79
5	20	1	2.5	0.5
6	40	1	4.0	0.72
7	20	2	4.0	0.61
8	40	2	2.5	0.71
9	20	2	1.0	0.51
10	60	2	4.0	0.89
11	60	1	2.5	0.78
12	20	3	2.5	0.55
13	40	3	1.0	0.61
14	40	1	1.0	0.56
15	40	2	2.5	0.70

Table 3 The result of the analysis of variance

Sources of variance	Statistical characteristics	
	F ratio	*P* value
X_1	227.80	0.0000
X_2	15.27	0.0113
X_3	67.57	0.0004
X_1^2	0.18	0.6870
X_1X_2	1.78	0.2397
X_1X_3	1.78	0.2397
X_2^2	1.80	0.2370
X_2X_3	0.15	0.7187
X_3^3	1.80	0.2370
Df	14	
R^2	97.1	
R^2_{adj}	94.6	

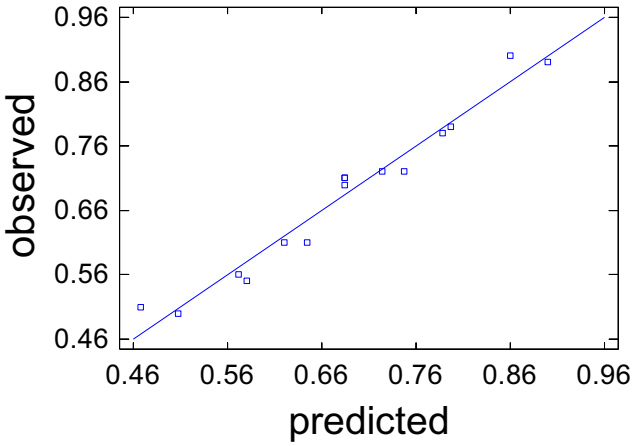

Fig. 3 The results of observations against the values of the output parameter Y_1 predicted by the mathematical model (1)

basic set of 6-31 + G (d, p). In the DFT methods, the Becke three-parameter exact exchange-functional functional (B3) [29] in combination with the correlation-corrected functional with the PW91 gradient is the best prediction result for molecular geometry and vibrational wavenumbers for a moderately larger molecule [30]. All calculations were obtained by adding a polarization function and a diffuse function on heavy atoms and a polarization and diffuse function on hydrogen atoms [31]. The Gaussian 09W program [32] was used with the B3PW91/6-31+G(d, p) basis set by the DFT approach where accurate structural and chemical properties can be obtained. Optimized structure with parameters of crystal, electrostatic potential energy map (MEP), and HOMO-LUMO molecular orbital analysis has been performed using Gauss View 5.0 [33]. Additionally, reactivities and behaviors of the studied products were predicted by using calculations of frontier orbitals and the chemical potential (μ), softness (S), chemical hardness (η), electron affinity (A), ionization energy (I), electronegativity (χ), and electrophilicity index (ω) [34–36].

Results and discussion

Synthesis of guar gum sulfate and BBD analysis

Sulfation of guar gum with complex of sulfur trioxide with 1,4-dioxane and of guar gum sulfate was carried out according to the scheme (Fig. 1).

In the study of guar gum sulfation by a complex of sulfur trioxide with 1,4-dioxane, the duration, process temperature, and amount of chlorosulfonic acid (for obtaining a complex of sulfur trioxide with 1,4-dioxane) were varied.

Two factors are included in the study as independent variables (in parentheses the levels of their variation): X_1, temperature (20, 40, 60 °C); X_2, the duration of the process of sulfation of guar gum (1.0, 2.0, 3.0 h), and X_3, volume of chlorosulfonic acid (to obtain a sulfating complex) (1.0, 2.5, 4.0 ml). The output parameter Y_1—degree

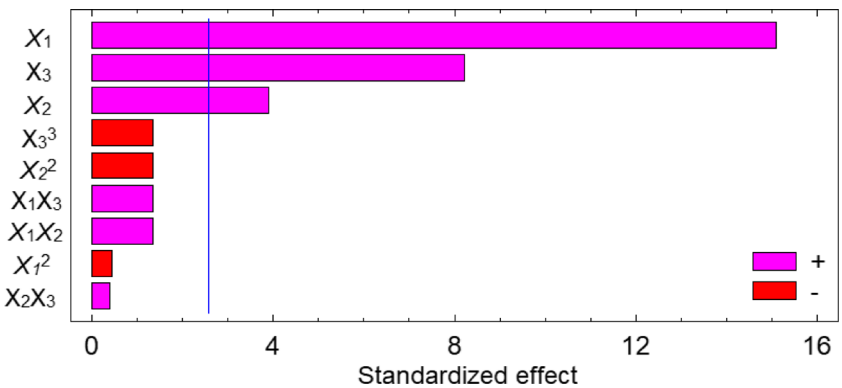

Fig. 2 Pareto analysis data of guar gum sulfation process with sulfur trioxide-1,4-dioxane complex

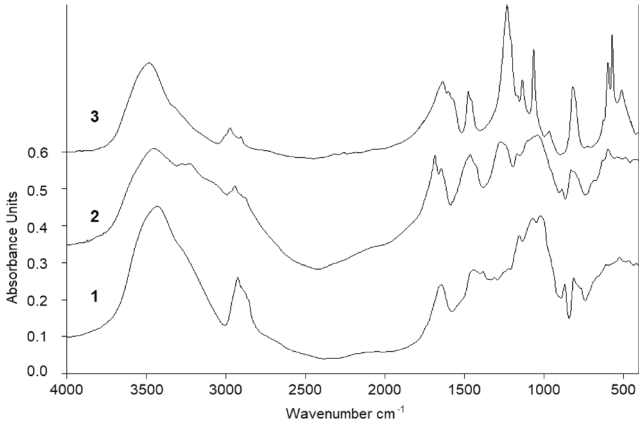

Fig. 4 FTIR spectra: 1, initial guar gum; 2, ammonium salt of guar gum sulfate; 3, sodium salt of guar gum sulfate

of substitution (DS)—was used as the result of the guar gum sulfation reaction. The Box-Behnken design (BBD) experiment plan was used. Each experiment was carried out in two parallels. The designations of the variables are given in Table 1.

The experimental results are shown in Table 2.

The dependence of the output parameter (Y_1) on variable process factors was approximated equations (2). The results of the analysis of variance are given in Table 3 and Fig. 2.

Analysis of variance showed within the limits of the accepted conditions, the factor—the temperature of the process of sulfation of guar gum—makes the greatest contribution to the total dispersion of the output parameter. This is characterized by high values of the dispersion F ratios for the main effects, also called influence efficiencies. The information contained in columns P of the table is interpreted similarly (Table 3).

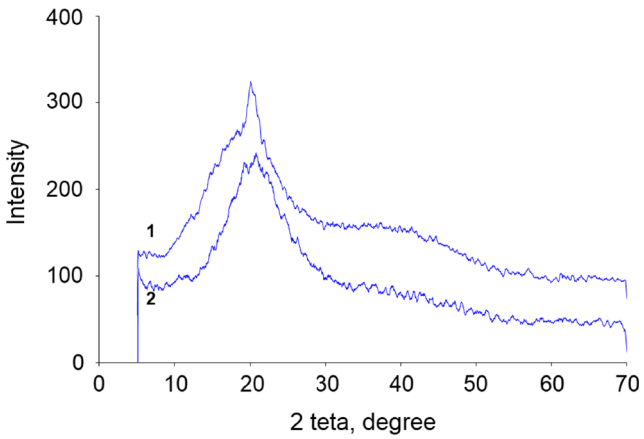

Fig. 5 X-ray diffraction spectra: 1, initial guar gum; 2, sodium salt of guar gum sulfate

The dependence of the degree of substitution in guar gum sulfates (Y_1) on variable process factors is approximated by the regression equation (2):

$$Y_1 = 0.224491 + 0.004958X_1 + 0.0663X_2 + 0.06157X_3 - 0.0000146X_1^2 + 0.0009X_1X_2 + 0.00058X_1X_3 - 0.018X_2^2 + 0.003X_2X_3 - 0.00815X_3^2 \quad (2)$$

The prognostic properties of Eq. (2) are demonstrated in Fig. 3, which compares the values of the output parameter Y_1 obtained in the experiment with the values calculated by Eq. (2). A straight line corresponds to the calculated values of Y_1, points—to the results of observations. The proximity of the "experimental points" to the line confirms the good prognostic properties of Eq. (2).

The quality of the approximation is also characterized by the coefficient of determination R^2_{adj}. In the considered problem, the value of $R^2_{adj} = 94.6\%$, which indicates a good quality of the approximation. This indicates the adequacy of Eq. (2) to the observation results and allows using it as a mathematical model of the process under study.

Optimal conditions for sulfation of guar gum with a complex of sulfur trioxide-1.4-dioxane are temperature 60 °C, duration 2.9 h, and a volume of chlorosulfonic acid of 3.1 ml.

FTIR spectroscopy

The initial and sulfated guar gum was analyzed by FTIR spectroscopy (Fig. 4).

FTIR spectra of sulfated guar gum show there is an intensity band at 1256 cm^{-1} (υ_{as} (O=S=O)) (Fig. 4). Absorption bands in the regions of 802–817 cm^{-1} and 855–867 cm^{-1} indicate the presence of sulfated groups in sulfated guar gum. FTIR spectra of sulfated guar gum show decreased the intensity of the absorption band of OH groups in the regions of 3419–3427 cm^{-1} and 1370–1380 cm^{-1}, which indicates a decrease in the number of OH groups in the sulfated product, due to their replacement with SO_3 groups.

The FTIR spectrum of the ammonium salt of sulfated guar gum differs from the spectrum of sodium salt (Fig. 4). FTIR spectrum shows there is a high-intensity band at 1260 cm^{-1}, corresponding υ_{as} (O=S=O). The absorption bands in the region of 3427–2930 cm^{-1}, (O–H and C–H bonds) broaden due to the superposition of the absorption bands of vibrations of N–H bonds in the ammonium cation. In the FTIR spectrum of the ammonium salt, in contrast to the sodium salt, there is an intense absorption band at 1447 cm^{-1}, corresponding to vibrations of the N–H bonds of the ammonium cation.

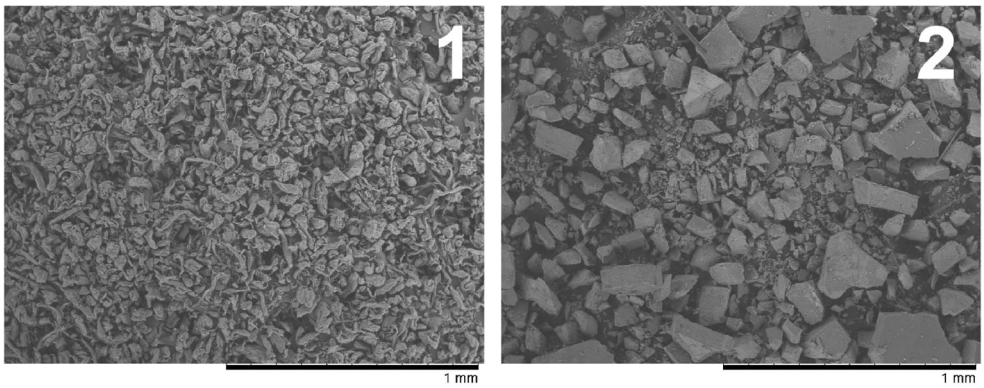

Fig. 6 SEM images of (1) the initial guar gum and (2) sulfated guar gum samples

X-ray diffractions

The initial and sulfated guar gum was analyzed by X-ray diffraction (Fig. 5).

Guar gum samples have an amorphous structure [37]. Comparison of X-ray diffraction patterns of the samples of guar gum and sodium salt of guar gum sulfate showed (Fig. 5) that further slight amorphization of the material structure occurs upon sulfation. On the X-ray diffraction pattern of the sodium salt of guar gum sulfate, smoothing of peaks was observed in the range of angles from 12 to 30° 2 (Fig. 5).

Scanning electron microscopy

According to scanning electron microscopy, the morphology of the samples changes during the sulfation of guar gum. Before the sulfation process, the guar gum sample consists of particles with an average size of 200 to 800 μm (Fig. 6 (1)). The introduction of a sulfate group into the guar gum molecule leads to a change in the average particle size from 80 to 1200 μm (Figure 6 (2)).

Gel permeation chromatography

According to the molecular mass distribution of guar gum (Table 4), the initial sample is guar gum with a molecular mass of ~ 600 kDa, which is consistent with the results presented in [38]. At the same time, GG has a bimodal mass distribution of particles: a high molecular weight fraction with an MM of ~ 1500 kDa and a low molecular weight fraction with an MM of ~ 600 kDa.

Table 4 Number-average molecular weight (M_n), weight-average molecular weight (M_w), and polydispersity of the galactomannan samples

Sample	M_n (kDa)	M_w (kDa)	PD
Guar gum	481.99	748.85	1.55
Sulfated guar gum	66.40	176.18	26.53

After the sulfation process, a redistribution of molecular masses in the sample is observed. The peak of the low molecular weight fraction with an MM of ~ 600 kDa disappears, and a new peak appears, corresponding to the product of the reaction with an MM of ~ 115 kDa. The fraction of the high molecular weight fraction in the sample also decreases markedly (Fig. 7), which is probably due to the partial destruction of GG and the ongoing competing hydrolysis reactions.

Galactomannan from guar gum is consisting of α-(1–6)-D-galactose and β-(1–4)-D-mannose [4, 5]. The conformation of the 1 → 4-linked backbone of β-D-mannan (as in cellulose), which makes it insoluble in water. However, the lateral galactose groups sterically disrupt interchain association thus increase the degree of solubility in water of galactomannans. As a result, the solubility of galactomannans increases with the degree of substitution of galactose: fenugreek and guar gum dissolve in cold water [5]. Thus, it can be assumed that upon sulfation of guar gum with a complex of sulfur trioxide and 1,4-dioxane, competing hydrolysis reactions take place along α-(1–6) bonds and cleavage of galactose units. This explains the production of both soluble guar gum sulfate and a small amount of insoluble residue.

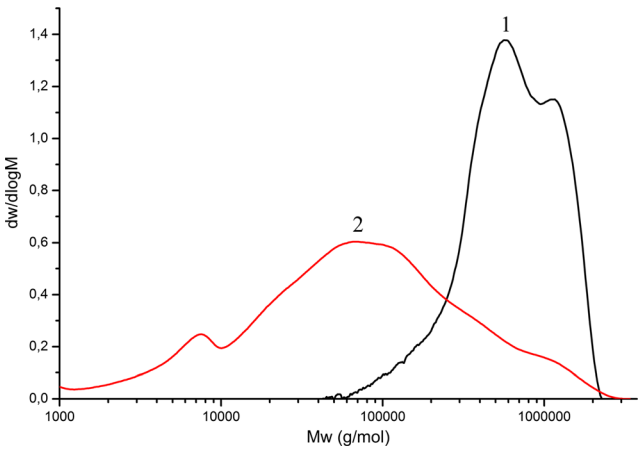

Fig. 7 Molecular weight distribution of guar gum (1) and sulfated guar gum (2) samples

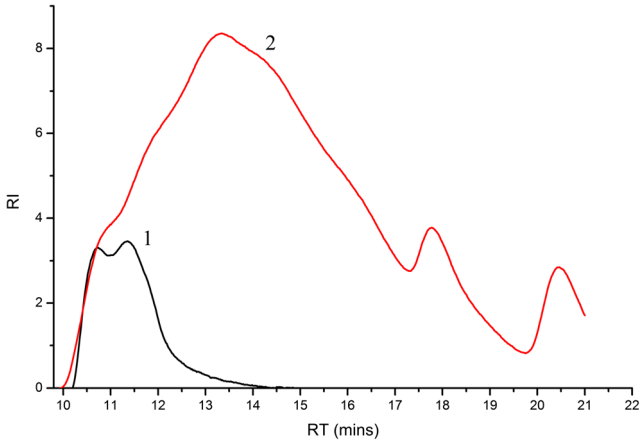

Fig. 8 Gel chromatogram of guar gum (1) and sulfated guar gum (2) samples

The peak with RT ~ 10.5 min (corresponding to the maximum mass) belongs to the unreacted guar gum (Fig. 8). The main peak Mw 176 kDa relates to the target product. Moreover, several peaks can be observed that can correspond to products of joint destruction and sulfation.

Molecular mass distribution may indicate different reactivity of individual sections of the guar gum chains (Fig. 8). Peaks with a release time of more than 17 min and a mass of less than 1 kDa are low molecular weight products of the destruction of guar gum.

Structural analyses

To determine the structural stability of the molecule under investigation, molecular optimization study was made by using a DFT calculation. The optimized molecular structure of pure gum (a), sulfated gum 1 (b), sulfated gum3 (c), and sulfated gum 5 (d) are represented in Fig. 9.

The SCF energy of these molecules are found to be − 1297.5124, − 2082.9407, − 3653.7564, and − 5224.6513 hartree, they belong to the C1 point group. The structural

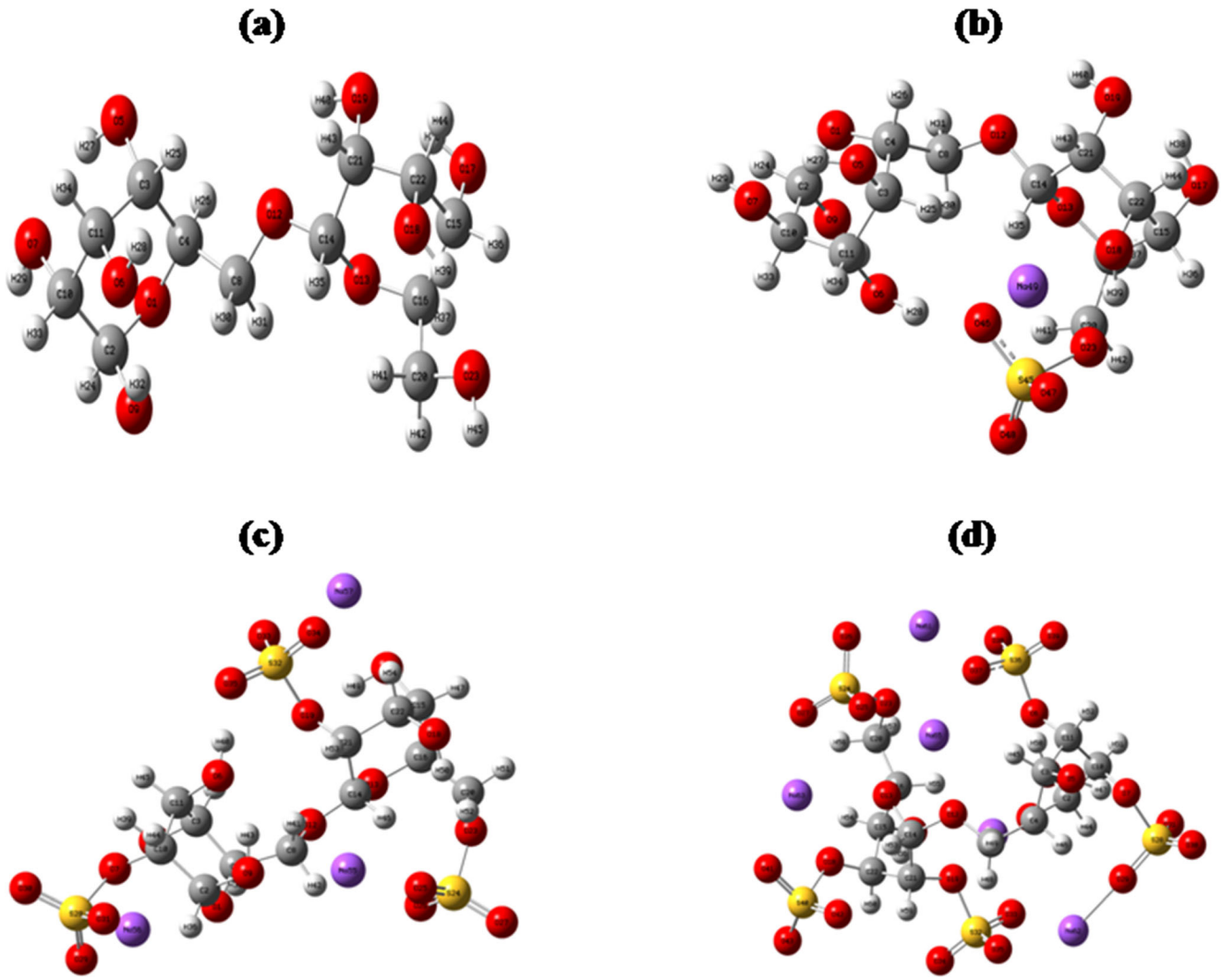

Fig. 9 Optimized molecular structures of **a** pure gum, **b** sulfated gum 1, **c** sulfated gum 3, **d** sulfated gum 5, as tube bond type

Table 5 Optimized bond lengths (Å) and bond angles (°) of pure gum and sulfated gum 1

Parameters	Pure gum	Parameters	Sulfated gum 1
Bond lengths (Å)			
O1–C2	1.4109	O1–C2	1.4137
O1–C4	1.429	O1–C4	1.4282
C2–O9	1.3996	C2–O9	1.3959
C2–C10	1.5379	C2–C10	1.5379
C2–H24	1.0968	C2–H24	1.0973
C3–C4	1.5392	C3–C4	1.5389
C3–O5	1.415	C3–O5	1.4179
C3–C11	1.5403	C3–C11	1.5431
C3–H25	1.097	C3–H25	1.0954
C4–C8	1.531	C4–C8	1.5377
C4–H26	1.0948	C4–H26	1.0951
O5–H27	0.9705	O5–H27	0.9714
O6–C11	1.4297	O6–C11	1.419
O6–H28	0.9643	O6–H28	0.9785
O7–C10	1.4229	O7–C10	1.4253
O7–H29	0.9647	O7–H29	0.9647
C8–O12	1.4284	C8–O12	1.4374
C8–H30	1.0964	C8–H30	1.0916
C8–H31	1.0938	C8–H31	1.0926
O9–H32	0.9711	O9–H32	0.9743
C10–C11	1.5307	C10–C11	1.5303
C10–H33	1.0985	C10–H33	1.098
C11–H34	1.0977	C11–H34	1.0988
O12–C14	1.3951	O12–C14	1.389
O13–C14	1.4175	O13–C14	1.4177
O13–C16	1.4308	O13–C16	1.4277
C14–C21	1.5294	C14–C21	1.5275
C14–H35	1.102	C14–H35	1.0996
C15–C16	1.5383	C15–C16	1.5487
C15–O17	1.4118	C15–O17	1.4122
C15–C22	1.5353	C15–C22	1.5468
C15–H36	1.0947	C15–H36	1.0973
C16–C20	1.5424	C16–C20	1.5379
C16–H37	1.0936	C16–H37	1.0954
O17–H38	0.9722	O17–H38	0.9725
O18–C22	1.4207	O18–C22	1.4313
O18–H39	0.9702	O18–H39	0.9804
O19–C21	1.4206	O19–C21	1.4171
O19–H40	0.9684	O19–H40	0.9693
C20–O23	1.4303	C20–O23	1.4452
C20–H41	1.0959	C20–H41	1.0938
C20–H42	1.0968	C20–H42	1.0942
C21–C22	1.5317	C21–C22	1.5295
C21–H43	1.0996	C21–H43	1.1017
C22–H44	1.0988	C22–H44	1.0953
O23–H45	0.9636	O23–S45	1.6746
		S45–O46	1.5084
		S45–O47	1.4798
		S45–O48	1.45
		O47–Na49	2.3345
Bond angles (°)			
C2–O1–C4	118.0201	C2–O1–C4	117.5593
O1–C2–O9	114.378	O1–C2–O9	114.0617
O1–C2–C10	111.0874	O1–C2–C10	110.6849
O1–C2–H24	103.3438	O1–C2–H24	103.2691
O9–C2–C10	111.2496	O9–C2–C10	111.323
O9–C2–H24	106.1605	O9–C2–H24	106.732
C10–C2–H24	110.165	C10–C2–H24	110.3712
C4–C3–O5	111.4698	C4–C3–O5	111.8904
C4–C3–C11	113.123	C4–C3–C11	113.0131
C4–C3–H25	107.5172	C4–C3–H25	107.7126
O5–C3–C11	109.6458	O5–C3–C11	110.2598
O5–C3–H25	105.7432	O5–C3–H25	105.5988
C11–C3–H25	109.0267	C11–C3–H25	107.9816
O1–C4–C3	113.1924	O1–C4–C3	112.8831
O1–C4–C8	110.7326	O1–C4–C8	111.6647
O1–C4–H26	104.3377	O1–C4–H26	104.2102
C3–C4–C8	115.4604	C3–C4–C8	114.7717
C3–C4–H26	105.598	C3–C4–H26	106.2131
C8–C4–H26	106.5146	C8–C4–H26	106.116
C3–O5–H27	107.2333	C3–O5–H27	106.7558
C11–O6–H28	109.409	C11–O6–H28	109.3182
C10–O7–H29	109.441	C10–O7–H29	109.3529
C4–C8–O12	106.9505	C4–C8–O12	108.4724
C4–C8–H30	112.8858	C4–C8–H30	113.6765
C4–C8–H31	108.4064	C4–C8–H31	108.5948
O12–C8–H30	109.1936	O12–C8–H30	109.8493
O12–C8–H31	110.6216	O12–C8–H31	107.8133
H30–C8–H31	108.7796	H30–C8–H31	108.272
C2–O9–H32	108.5974	C2–O9–H32	108.1849
C2–C10–O7	111.6376	C2–C10–O7	111.6006
C2–C10–C11	110.5315	C2–C10–C11	110.0758
C2–C10–H33	108.7265	C2–C10–H33	108.8668
O7–C10–C11	105.8362	O7–C10–C11	106.2811
O7–C10–H33	110.7789	O7–C10–H33	110.7471
C11–C10–H33	109.2953	C11–C10–H33	109.2286
C3–C11–O6	112.7635	C3–C11–O6	112.5776
C3–C11–C10	110.8166	C3–C11–C10	110.2872
C3–C11–H34	108.1151	C3–C11–H34	107.9628
O6–C11–C10	105.7779	O6–C11–C10	106.2821
O6–C11–H34	110.5767	O6–C11–H34	110.9983
C10–C11–H34	108.7347	C10–C11–H34	108.6823
C8–O12–C14	114.9311	C8–O12–C14	116.9648
C14–O13–C16	115.9752	C14–O13–C16	116.4151
O12–C14–O13	107.5234	O12–C14–O13	108.0909
O12–C14–C21	106.6072	O12–C14–C21	106.1054

Table 5 (continued)

Parameters	Pure gum	Parameters	Sulfated gum 1
O12–C14–H35	110.2543	O12–C14–H35	111.5615
O13–C14–C21	112.7563	O13–C14–C21	111.2736
O13–C14–H35	110.432	O13–C14–H35	109.1457
C21–C14–H35	109.1805	C21–C14–H35	110.6224
C16–C15–O17	110.6406	C16–C15–O17	110.0554
C16–C15–C22	111.2255	C16–C15–C22	113.7099
C16–C15–H36	108.1785	C16–C15–H36	108.873
O17–C15–C22	111.2048	O17–C15–C22	108.9151
O17–C15–H36	106.2312	O17–C15–H36	106.1225
C22–C15–H36	109.1783	C22–C15–H36	108.8818
O13–C16–C15	111.2437	O13–C16–C15	111.5381
O13–C16–C20	109.9847	O13–C16–C20	114.0924
O13–C16–H37	104.086	O13–C16–H37	103.0247
C15–C16–C20	115.6718	C15–C16–C20	116.5703
C15–C16–H37	105.8028	C15–C16–H37	105.0604
C20–C16–H37	109.3136	C20–C16–H37	104.8899
C15–O17–H38	107.3529	C15–O17–H38	107.2235
C22–O18–H39	108.8347	C22–O18–H39	106.7256
C21–O19–H40	107.0731	C21–O19–H40	106.914
C16–C20–O23	109.3608	C16–C20–O23	113.3887
C16–C20–H41	110.0212	C16–C20–H41	109.4013
C16–C20–H42	109.0441	C16–C20–H42	109.2285
O23–C20–H41	109.7742	O23–C20–H41	110.5204
O23–C20–H42	110.5042	O23–C20–H42	105.7306
H41–C20–H42	108.1194	H41–C20–H42	108.4022
C14–C21–O19	110.7739	C14–C21–O19	110.685
C14–C21–C22	110.3748	C14–C21–C22	110.2826
C14–C21–H43	108.0124	C14–C21–H43	108.4328
O19–C21–C22	108.1133	O19–C21–C22	107.9411
O19–C21–H43	110.6347	O19–C21–H43	110.3877
C22–C21–H43	108.9215	C22–C21–H43	109.1011
C15–C22–O18	112.2121	C15–C22–O18	113.2414
C15–C22–C21	110.2165	C15–C22–C21	110.4509
C15–C22–H44	108.403	C15–C22–H44	107.0531
O18–C22–C21	106.7207	O18–C22–C21	108.7202
O18–C22–H44	110.7016	O18–C22–H44	108.2778
C21–C22–H44	108.5286	C21–C22–H44	108.9943
C20–O23–H45	109.0795	C20–O23–S45	120.2504
		O23–S45–O46	103.7042
		O23–S45–O47	99.0942
		O23–S45–O48	107.6773
		O46–S45–O47	108.7955
		O46–S45–O48	115.2215
		O47–S45–O48	119.8288
		S45–O47–Na49	93.3444

Table 6 Optimized bond lengths (Å) and bond angles (°) of sulfated gum 3 and sulfated gum 5

Parameters	Sulfated gum 3	Parameters	Sulfated gum 5
Bond lengths (Å)			
O1–C2	1.4532	O1–C2	1.4291
O1–C4	1.4261	O1–C4	1.4335
C2–O9	1.3878	C2–O9	1.4103
C2–C10	1.5385	C2–C10	1.5338
C2–H36	1.0912	C2–H44	1.0919
C3–C4	1.5297	C3–C4	1.551
C3–O5	1.4376	C3–O5	1.4069
C3–C11	1.5464	C3–C11	1.5417
C3–H37	1.097	C3–H45	1.0937
C4–C8	1.5311	C4–C8	1.5205
C4–H38	1.0992	C4–H46	1.0971
O5–H39	0.9663	O5–H47	0.9713
O6–C11	1.4189	O6–C11	1.4496
O6–H40	0.9778	O6–S36	1.6715
O7–C10	1.415	O7–C10	1.4226
O7–S28	1.757	O7–S28	1.7179
C8–O12	1.4397	C8–O12	1.4379
C8–H41	1.0887	C8–H48	1.0898
C8–H42	1.096	C8–H49	1.0974
O9–H43	0.9715	O9–H50	0.9743
C10–C11	1.5349	C10–C11	1.5319
C10–H44	1.0957	C10–H51	1.0955
C11–H45	1.0996	C11–H52	1.0936
O12–C14	1.4062	O12–C14	1.4151
O13–C14	1.417	O13–C14	1.4215
O13–C16	1.4433	O13–C16	1.4304
C14–C21	1.5304	C14–C21	1.5533
C14–H46	1.1018	C14–H53	1.0955
C15–C16	1.5344	C15–C16	1.5429
C15–O17	1.4413	C15–O17	1.4291
C15–C22	1.5405	C15–C22	1.5442
C15–H47	1.0939	C15–H54	1.0978
C16–C20	1.5329	C16–C20	1.5207
C16–H48	1.0946	C16–H55	1.0975
O17–H49	0.9749	O17–H56	0.966
O18–C22	1.4124	O18–C22	1.4181
O18–H50	0.9645	O18–S40	1.7477
O19–C21	1.4323	O19–C21	1.431
O19–S32	1.6769	O19–S32	1.6865
C20–O23	1.4137	C20–O23	1.4282
C20–H51	1.0964	C20–H57	1.0944
C20–H52	1.0956	C20–H58	1.094
C21–C22	1.5475	C21–C22	1.5457
C21–H53	1.0955	C21–H59	1.0921
C22–H54	1.09	C22–H60	1.0975
O23–S24	1.6921	O23–S24	1.7162
S24–O25	1.4967	S24–O25	1.4768

Table 6 (continued)

Parameters	Sulfated gum 3	Parameters	Sulfated gum 5
S24–O26	1.487	S24–O26	1.4698
S24–O27	1.4515	S24–O27	1.4747
O25–Na55	2.399	O25–Na61	3.5778
S28–O29	1.4934	O25–Na65	2.2632
S28–O30	1.4565	S28–O29	1.5012
S28–O31	1.464	S28–O30	1.4517
O29–Na56	2.2367	S28–O31	1.4645
S32–O33	1.481	O29–Na62	2.1618
S32–O34	1.4868	S32–O33	1.4995
S32–O35	1.4639	S32–O34	1.4527
O33–Na57	2.3535	S32–O35	1.4816
		O33–Na64	2.318
		S36–O37	1.5057
		S36–O38	1.482
		S36–O39	1.452
		O37–Na65	2.2461
		O38–Na61	2.3348
		S40–O41	1.4848
		S40–O42	1.4711
		S40–O43	1.4544
		O41–Na63	2.2549
		H46–Na62	3.1522
		H58–Na63	3.0007
Bond angles (°)			
C2–O1–C4	116.2467	C2–O1–C4	118.6817
O1–C2–O9	111.9623	O1–C2–O9	105.967
O1–C2–C10	109.5371	O1–C2–C10	112.3051
O1–C2–H36	103.1639	O1–C2–H44	109.7195
O9–C2–C10	112.3261	O9–C2–C10	112.7802
O9–C2–H36	108.7036	O9–C2–H44	105.5565
C10–C2–H36	110.7754	C10–C2–H44	110.2131
C4–C3–O5	104.4919	C4–C3–O5	110.0258
C4–C3–C11	112.5651	C4–C3–C11	111.5783
C4–C3–H37	109.3232	C4–C3–H45	111.0777
O5–C3–C11	112.1287	O5–C3–C11	112.4224
O5–C3–H37	109.534	O5–C3–H45	104.7675
C11–C3–H37	108.7053	C11–C3–H45	106.725
O1–C4–C3	111.1066	O1–C4–C3	112.7205
O1–C4–C8	112.7408	O1–C4–C8	107.4026
O1–C4–H38	104.4404	O1–C4–H46	109.3036
C3–C4–C8	115.504	C3–C4–C8	113.227
C3–C4–H38	106.0492	C3–C4–H46	106.7528
C8–C4–H38	105.9963	C8–C4–H46	107.262
C3–O5–H39	108.8004	C3–O5–H47	107.0188
C11–O6–H40	109.7336	C11–O6–S36	119.0719
C10–O7–S28	119.5053	C10–O7–S28	119.616
C4–C8–O12	106.1307	C4–C8–O12	108.2953
C4–C8–H41	111.6507	C4–C8–H48	110.5705
C4–C8–H42	109.6625	C4–C8–H49	108.641

Table 6 (continued)

Parameters	Sulfated gum 3	Parameters	Sulfated gum 5
O12–C8–H41	110.022	O12–C8–H48	110.8855
O12–C8–H42	110.3063	O12–C8–H49	109.5027
H41–C8–H42	109.0437	H48–C8–H49	108.9095
C2–O9–H43	108.8354	C2–O9–H50	106.8542
C2–C10–O7	111.7955	C2–C10–O7	112.8861
C2–C10–C11	110.0033	C2–C10–C11	108.7183
C2–C10–H44	108.649	C2–C10–H51	108.4242
O7–C10–C11	105.6018	O7–C10–C11	103.3585
O7–C10–H44	111.0561	O7–C10–H51	110.8846
C11–C10–H44	109.7015	C11–C10–H51	112.5575
C3–C11–O6	109.8452	C3–C11–O6	110.5519
C3–C11–C10	112.0865	C3–C11–C10	109.3823
C3–C11–H45	109.1542	C3–C11–H52	109.5848
O6–C11–C10	107.1493	O6–C11–C10	106.605
O6–C11–H45	110.6911	O6–C11–H52	109.6385
C10–C11–H45	107.8931	C10–C11–H52	111.0449
C8–O12–C14	114.1703	C8–O12–C14	121.8486
C14–O13–C16	116.0494	C14–O13–C16	113.5854
O12–C14–O13	102.7136	O12–C14–O13	102.9542
O12–C14–C21	114.7363	O12–C14–C21	117.2976
O12–C14–H46	108.7325	O12–C14–H53	111.4406
O13–C14–C21	109.7855	O13–C14–C21	111.4736
O13–C14–H46	110.1394	O13–C14–H53	105.3884
C21–C14–H46	110.453	C21–C14–H53	107.6578
C16–C15–O17	109.2575	C16–C15–O17	106.7954
C16–C15–C22	113.0194	C16–C15–C22	109.3124
C16–C15–H47	109.6896	C16–C15–H54	110.1749
O17–C15–C22	109.4822	O17–C15–C22	115.6435
O17–C15–H47	106.2145	O17–C15–H54	108.905
C22–C15–H47	108.9504	C22–C15–H54	105.987
O13–C16–C15	109.8882	O13–C16–C15	110.9074
O13–C16–C20	112.8312	O13–C16–C20	107.2551
O13–C16–H48	103.4206	O13–C16–H55	107.8407
C15–C16–C20	116.4633	C15–C16–C20	111.7727
C15–C16–H48	107.2818	C15–C16–H55	109.4204
C20–C16–H48	105.8773	C20–C16–H55	109.5438
C15–O17–H49	105.3639	C15–O17–H56	108.6667
C22–O18–H50	111.9166	C22–O18–S40	121.8379
C21–O19–S32	121.6899	C21–O19–S32	119.1656
C16–C20–O23	108.6981	C16–C20–O23	111.2154
C16–C20–H51	108.7659	C16–C20–H57	109.5581
C16–C20–H52	113.4016	C16–C20–H58	111.0945
O23–C20–H51	107.455	O23–C20–H57	107.5308
O23–C20–H52	110.2178	O23–C20–H58	109.088
H51–C20–H52	108.1253	H57–C20–H58	108.2415
C14–C21–O19	105.0469	C14–C21–O19	110.069
C14–C21–C22	107.9764	C14–C21–C22	108.4487
C14–C21–H53	111.3961	C14–C21–H59	108.9138
O19–C21–C22	111.4556	O19–C21–C22	107.4761

Table 6 (continued)

Parameters	Sulfated gum 3	Parameters	Sulfated gum 5
O19–C21–H53	111.5454	O19–C21–H59	110.988
C22–C21–H53	109.3189	C22–C21–H59	110.9065
C15–C22–O18	113.2857	C15–C22–O18	102.4049
C15–C22–C21	109.914	C15–C22–C21	109.5423
C15–C22–H54	108.5725	C15–C22–H60	110.9717
O18–C22–C21	112.1896	O18–C22–C21	113.6411
O18–C22–H54	104.7891	O18–C22–H60	111.4395
C21–C22–H54	107.7666	C21–C22–H60	108.7313
C20–O23–S24	119.1207	C20–O23–S24	118.7492
O23–S24–O25	103.78	O23–S24–O25	103.4626
O23–S24–O26	100.5833	O23–S24–O26	98.9761
O23–S24–O27	106.1702	O23–S24–O27	105.6089
O25–S24–O26	110.1072	O25–S24–O26	114.7127
O25–S24–O27	116.5032	O25–S24–O27	113.5142
O26–S24–O27	117.3316	O26–S24–O27	117.7457
S24–O25–Na55	87.9633	S24–O25–Na61	56.8116
O7–S28–O29	97.5816	S24–O25–Na65	111.4216
O7–S28–O30	102.8029	Na61–O25–Na65	71.9164
O7–S28–O31	104.0513	O7–S28–O29	101.6725
O29–S28–O30	114.7885	O7–S28–O30	101.1923
O29–S28–O31	115.2036	O7–S28–O31	104.4348
O30–S28–O31	118.2993	O29–S28–O30	113.9403
S28–O29–Na56	104.1746	O29–S28–O31	112.6755
O19–S32–O33	99.419	O30–S28–O31	119.8031
O19–S32–O34	105.7788	S28–O29–Na62	162.2827
O19–S32–O35	106.0634	O19–S32–O33	97.7199
O33–S32–O34	110.8855	O19–S32–O34	106.5325
O33–S32–O35	116.7023	O19–S32–O35	105.6349
O34–S32–O35	115.8492	O33–S32–O34	116.8211
S32–O33–Na57	90.5788	O33–S32–O35	110.1127
		O34–S32–O35	117.3638
		S32–O33–Na64	103.7354
		O6–S36–O37	104.5104
		O6–S36–O38	101.738
		O6–S36–O39	106.8459
		O37–S36–O38	108.5919
		O37–S36–O39	114.9897
		O38–S36–O39	118.3618
		S36–O37–Na65	134.1792
		S36–O38–Na61	97.038
		O18–S40–O41	95.2895
		O18–S40–O42	103.1673
		O18–S40–O43	105.3504
		O41–S40–O42	114.2381
		O41–S40–O43	117.0133
		O42–S40–O43	117.4096
		S40–O41–Na63	106.2702
		C4–H46–Na62	113.739
		C20–H58–Na63	112.3582

Table 6 (continued)

Parameters	Sulfated gum 3	Parameters	Sulfated gum 5
		O25–Na61–O38	123.2546
		O29–Na62–H46	50.4703
		O41–Na63–H58	135.5096
		O25–Na65–O37	104.6774

parameters of optimized geometries are computed by B3PW91 with a 6-31 + G (d, p) basis set. The bond lengths and angles of pure gum and sulfated gum 1 are listed in Table 5, whereas the calculated parameters of the two other compounds are tabulated in Table 6.

The comparison of the theoretical values of pure gum-sulfated gum 1 as well sulfated gum 3-sulfated gum 5 shows a slight difference owing to sulfation reaction. The bond length values are in the range 0.9636–1.5403 Å (pure gum) and 0.9693–2.3345 Å (sulfated gum 1); the longer bonds are C16–C20 and O47–Na49 and the shorter ones are O23–H45 and O19–H40, as it is shown in Table 5. Similarly for Table 2, the bond lengths are between 0.9645 and 2.3535 Å (sulfated gum 3), among 0.9660 and 3.5778 Å (sulfated gum 5). The longest and shortest bond lengths in the sulfated gum 3-sulfated gum 5 cases are O25–Na55/O25–Na61 and O18–H50/O17–H56. Concerning bond angles which ranging from 103.3438 to 118.0201 and from 93.3444 to 119.8288° for pure gum and sulfated gum 1, whereas for both other structures are in the interval 87.9633–121.68994° and 50.4703–135.5069°. As seen from Table 6, the largest angles are C2–O1–C4 (pure gum), O47–S45–O48 (sulfated gum 1), C21–O19–S32 (sulfated gum 3), and O41–Na63–H85 (sulfated gum 5). The O1–C2–H24, S45–O47–Na49, S24–O25–Na55, and O29–Na62–H46 bond angles are considered as the smallest ones for pure gum, sulfated gum, sulfated gum 3, and sulfated gum 5, respectively.

Frontier molecular orbitals

Frontier molecular orbitals, HOMO and LUMO, and the corresponding energies are highly significant in charge-transfer interaction analysis. The highest occupied molecular orbital (HOMO) possesses the ability to donor an electron, while the lowest unoccupied molecular orbital (LUMO) is considered like an electron acceptor owing to his ability to win an electron. In addition, a low frontier orbital gap magnitude indicates high chemical reactivity consequently low kinetic stability of the working compound [34]. The HOMO and LUMO orbitals of the studied compounds and their energy plots are illustrated in Fig. 10.

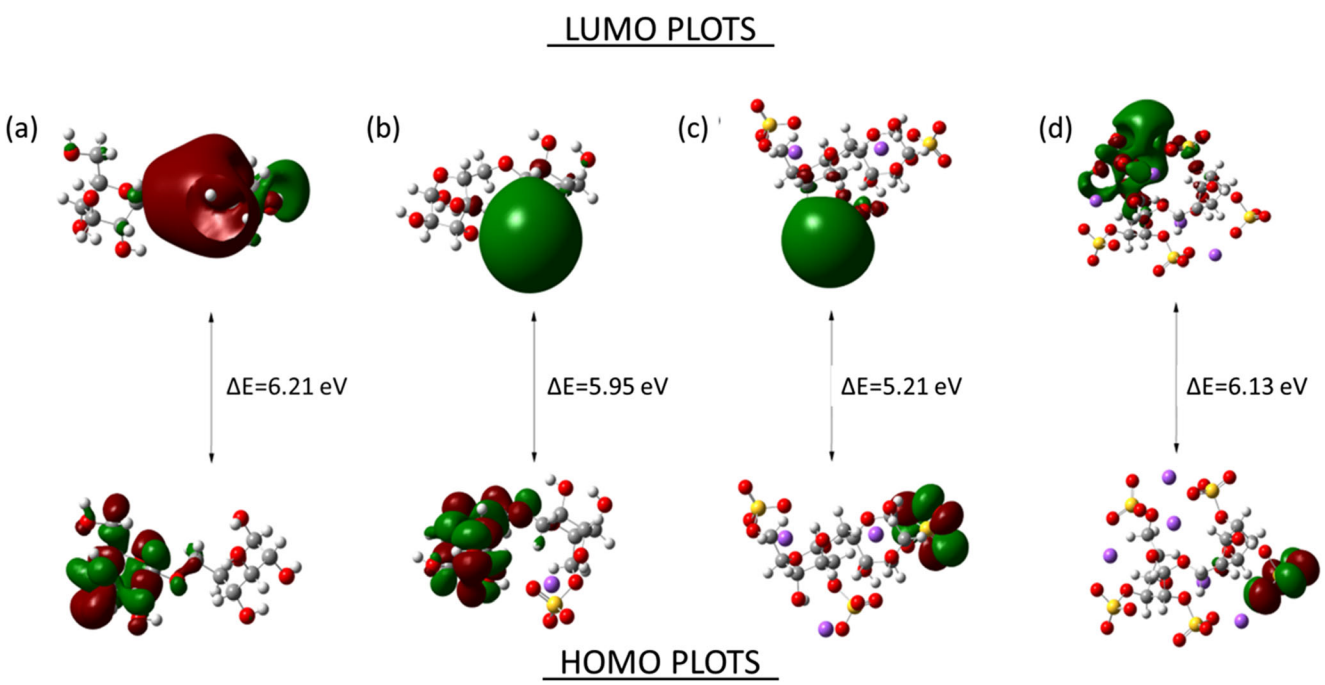

Fig. 10 HOMO-LUMO orbitals of **a** pure gum, **b** sulfated gum 1, **c** sulfated gum 3, **d** sulfated gum 5 and their energy gap

As clearly seen from this figure, there are two colors: the red color marks the positive phase and the green one associate with the negative region. The gap energy of the guar gum sulfates calculated at B3PW91/6-31 + G (d, p) level of theory is equal to 6.21 eV (pure gum), 5.95 eV (sulfated gum 1), 5.21 eV (sulfated gum 3), and 6.13 eV (sulfated gum 5). These computed energy values show that sulfated gum 3 molecule has the greatest electronic charge transfer since it mark the lowest energy band gap ΔE. In order to predict the chemical reactivity of the different species, several parameters are calculated throughout HOMO and LUMO energies and tabulated in Table 7.

The ionization energy (I) and electron affinity (A) are calculated via the following equations; $I = -E_{HOMO}$ and $A = -E_{LUMO}$. The electronegativity (χ) and chemical hardness (μ) are computed as follows; $\chi = (I + A)/2$ and $\eta = -(I + A)/2$, while the chemical potential, maximum charge transfer index, global softness, and electrophilicity index are defined as $\mu = -\chi$, $\Delta N_{max} = -\mu/\eta$, $\varsigma = 1/\eta$, and $\omega = \mu^2/2\eta$, respectively. The maximum charge transfer index is directly related to the gap energy, the lower HOMO-LUMO energy separation, the greater ΔN_{max}. Building on these two factors, the sulfated gum 3 molecule is considered the most reactive candidate compound since it has the weaker energy band gap (5.2180 eV) and the highest transfer index (1.6798). Compared to the other compounds, sulfated gum 3 has the largest electronic charge transfer flow between HOMO-LUMO orbitals, conversely for the most stable pure gum system with 3.3064 eV (chemical hardness)/0.3024 eV^{-1} (softness).

Table 7 Some electronic properties for pure gum and sulfated gums (1, 3, 5)

Parameters (eV)	Pure gum	Sulfated gum 1	Sulfated gum 3	Sulfated gum 5
E_{HOMO}	− 7.0262	− 7.1846	− 6.9916	− 7.5176
E_{LUMO}	− 0.4133	− 1.2324	− 1.7736	− 1.3831
Energy band gap (ΔE)	6.6129	5.9522	5.2180	6.1345
Chemical potential (μ)	− 3.7197	− 4.2085	− 4.3826	− 4.4503
Softness (ς)	0.3024	0.3360	0.3832	0.3260
Ionization energy (I)	7.0262	7.1846	6.9916	7.5176
Electron affinity (A)	0.4133	1.2324	1.7736	1.3831
Electronegativity (χ)	3.7197	4.2085	4.3826	4.4503
Chemical hardness (η)	3.3064	2.9761	2.6090	3.0672
Electrophilicity index (ω)	2.0922	2.9756	3.6809	3.2284
Maximum charge transfer index (ΔN_{max})	1.1250	1.4140	1.6798	1.4509

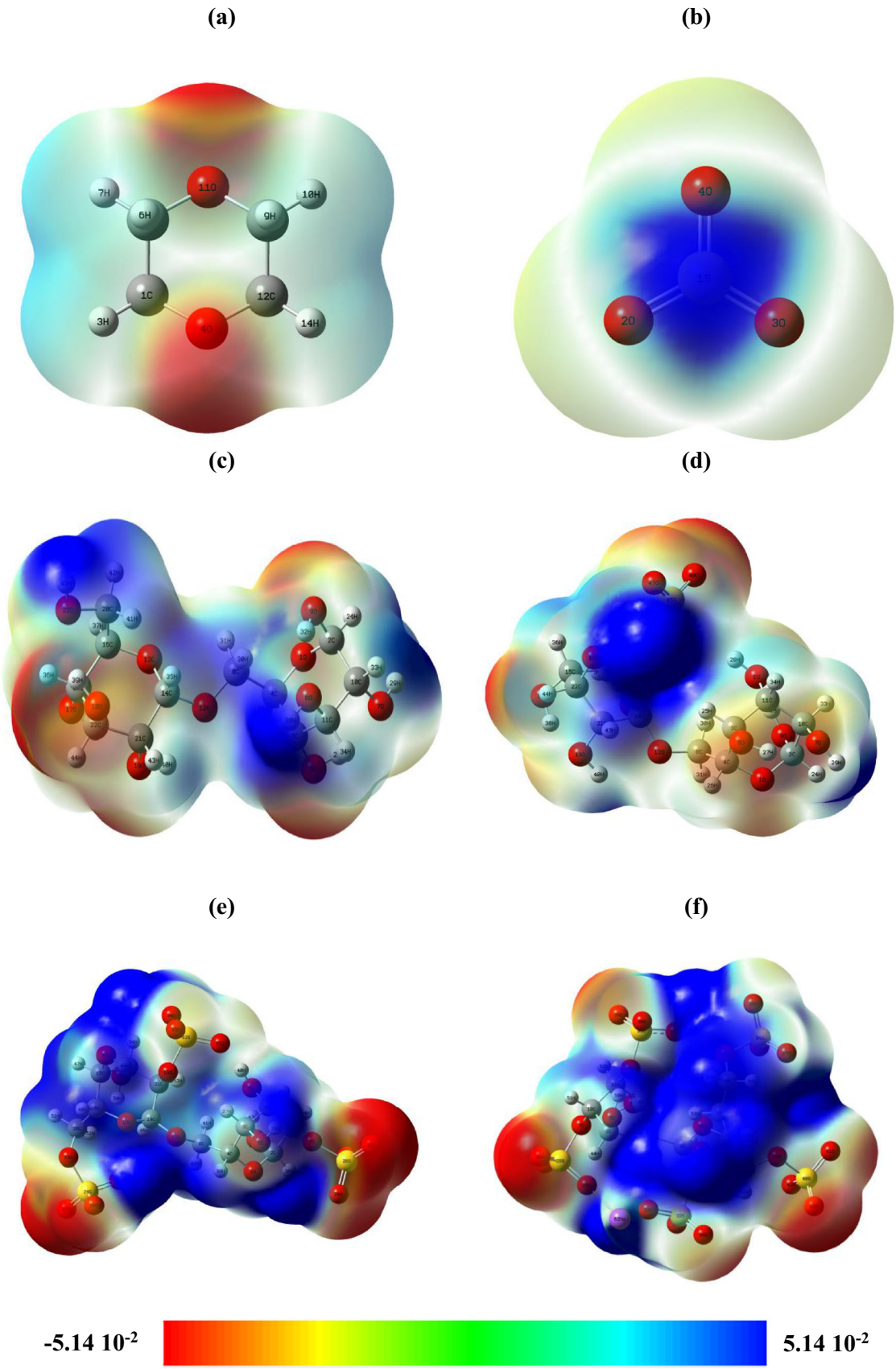

Fig. 11 MEP reactive regions of **a** 1,4-dioxane, **b** SO_3, **c** pure gum, **d** sulfated gum 1, **e** sulfated gum 3, **f** sulfated gum 5

Molecular electrostatic potential analysis

Molecular electrostatic potential (MEP) is widely used in the quantum molecular description. It provided a visual representation of charge distribution and enabled to define nucleophilic and electrophilic molecular sites; for this reason, it was employed in numerous studies [39–44]. MEP surface of 1,4-dioxane and SO_3 along with compounds under investigation is mapped with the help of the B3PW91/6-31 + G (d, p) method, as it is shown in Fig. 11.

In this schematical visualization, each electrostatic potential value is plotted by a color. The increasing order potential is as follows: red < orange < yellow < green < blue. The color code of the investigated molecule surfaces ranging from $-5.14 \cdot 10^{-2}$ (profoundest red) to $5.14 \cdot 10^{-2}$ (profoundest blue). The nucleophilic region is represented by red color, indicating strong repulsion (potential < 0), whereas the electrophilic area is planned with blue demonstrating strong attraction (potential > 0). The green is associated with the neutral region with zero potential value. As shown in Fig. 11a, the two oxygen atoms of the 1,4-dioxane molecule possess a negative potential (red color). Generally, the positive σ-hole potential is present in covalent groups as well as in halogen and hydrogen groups. In our case, despite the weak blue color intensity of hydrogen atoms localized at the edge of the surface, we can say that the hydrogen atoms have σ-hole electrostatic potential. Then, the positive sign of electrostatic potential is associated with σ-hole and π-holes which are used in intermolecular interactions explication [45–47]. Based on this fact, the SO_3 compound has a positive electrostatic potential value (Fig. 11b), so it a molecule with π-holes. As clearly seen in Fig. 11c–f, the hydrogen atoms connected to hydroxyl groups located at the interface of the maps have the weaker electronic density and are plotted by blue color, while the oxygen atoms of the same group possess the greatest electronic density and it is shown as red. The MEP surface of pure gum presents four electrophilic sites with a potential value equal to 0.1087 (H28), 0.1046 (H45), 0.1023 (H29), and 0.0436 a.u (H40). Relating to nucleophilic attacks, the electrostatic potential ranging from −0.0443 to −0.0771 a.u. Passing from pure gum to sulfated gum (1, 3, 5), the maps present some modifications. For sulfated molecules, the nucleophilic sites (red color) are concentrated not only on the oxygen atoms of the hydroxyl group but also on the oxygen of the sulfate groupment. On the other side, the blue color (electrophilic side) is localized mainly over sodium atoms. From the figure, we notice that the insertion of sulfated atoms in the pure gum increases the number of nucleophilic and electrophilic attacks which rise the chemical reactivity of the system.

Conclusions

For the first time, the synthesis of guar gum sulfates by a complex of sulfur trioxide with 1,4-dioxane was studied. The high degree of substitution (0.91) was achieved at a temperature of 60 °C, duration of 2.9 h, and a volume of chlorosulfonic acid of 3.1 ml.

The introduction of sulfate groups into the structure of guar gum was confirmed by elemental analysis, FTIR. The FTIR spectra of sulfated guar gum contain bands at 1260 cm^{-1} and 802–817 cm^{-1}, which indicate the presence of sulfate groups.

The initial and sulfated guar gum was also investigated by the methods: X-ray diffraction and gel permeation chromatography. Using X-ray diffraction showed that sulfation leads to partial amorphization of guar gum.

Using gel permeation chromatography, it was shown that in the process of guar gum sulfation by a complex of sulfur trioxide with 1,4-dioxane, the molecular weight decreases from 600 to 176 kDa.

The optimized structures of pure and sulfated (1, 3, 5) guar gum were obtained with the help of B3PW91 with a 6-31 + G (d, p) basis set. Building on the comparison made between the four geometries, there are differences between geometrical parameters (bond length and bong angle) due to sulfation reaction. HOMO-LUMO frontier orbital analysis proves that the sulfated gum 3 is the reactive compound compared to the other ones. In addition, the MEP contour maps show the effect of sulfation on the chemical reactivity of the system. These surfaces make out the proportionality between the sulfated atoms number and the molecular reactivity.

Acknowledgments The devices of the Krasnoyarsk Regional Center of Research Equipment of Federal Research Center "Krasnoyarsk Science Center SB RAS" were used in the work. The authors are grateful to G.N. Bondarenko for obtaining X-ray data, Korolkova I.V. for obtaining FTIR spectra and Antonov A.V. for obtaining SEM images. Besides, the authors thank Bitlis Eren University for supporting the Gaussian 09W software and Bingol University for the server.

Availability of data and material N/A.

Authors' contributions Conceptualization: Aleksandr S. Kazachenko, Feride Akman, Abir Sagaama, Noureddine Issaoui; methodology: Aleksandr S. Kazachenko, Feride Akman, Noureddine Issaoui; formal analysis and investigation: Feride Akman, Abir Sagaama, Noureddine Issaoui, Yuriy N. Malyar, Valentina S. Borovkova, Aleksandr S. Kazachenko; writing—original draft preparation: Noureddine Issaoui, Feride Akman, Abir Sagaama, Aleksandr S. Kazachenko; writing—review and editing: Aleksandr S. Kazachenko, Feride Akman, Abir Sagaama, Noureddine Issaoui; supervision: Feride Akman, Abir Sagaama, Noureddine Issaoui, Natalya Yu. Vasilieva.

Funding This work was supported by the Ministry of Higher Education and Scientific Research of Tunisia. The publication also supported by RFBR, project № 20-33-70256.

Compliance with ethical standards

Conflict of interest The authors declare that they have no conflict of interest.

Consent for publication N/A.

Ethics approval N/A. In the course of work on this article, the authors did not conduct research on animals and humans in any form.

Consent to participate N/A.

Code availability N/A.

References

1. Zhao X, Zhou H, Sikarwar VS, Zhao M, Park A-HA, Fennell PS, Shen L, Fan L-S (2017). Energy Environ Sci 10(9):1885–1910
2. Medvedeva EN, Babkin VA, Ostrouhova LA (2003). Chem Raw Plant Mater 1:27–37
3. Dushkin AV, Meteleva ES, Tolstikova TG, Pavlova AV, Khvostov MV (2013). Pharm Chem J 46(10):630–633
4. Cerqueira MA, Bourbon AI, Pinheiro AC, Martins JT, Souza BWS, Teixeira JA, Vicenta AA (2011). Trends Food Sci Technol 22:662–671
5. Prajapati VD, Jani GK, Moradiya NG, Randeria NP, Nagar BJ, Naikwadi NN, Variya BC (2013). Int J Biol Macromol 60:83–92
6. Filatova AV, Azimova LB, Turaev AS (2020). Chem Plant Raw Mater 1:33–39
7. Mercier T, Guldentops E, Lagrou K, Maertens J (2018). Front Microbiol 9:661
8. Perera N, Yang FL, Chang CM, Lu YT, Zhan SH, Tsai YT, Hsieh JF, Li LH, Hua KF, Wu SH (2017). Org Lett 19(13):3486–3489
9. Tolstenkov AS, Drozd NN, Lapikova EU, Makarov VA, Mestechkina NM, Bannikova GE, Ilyina AB, Varlamov VP (2007). Clinical Hematol Hemorheol in Cardiovasc Surgery 7: 242–243 (in Rus)
10. Mestechkina NM, Anulov OV, Scherbukhin VD (1998). Appl Biochem Microbiol (Rus) 34(5):549–552
11. Mestechkina NM, Dovletmuradov K, Scherbukhin VD (1991). Appl Biochem Microbiol (Rus) 27(3):435–441
12. Krishtanova NA, Safonova MJ, Bolotova VTS (2005). Proc Voronezh St Univ Ser: Chem Biol Pharm 1:212–221 (in Russ)
13. Mudgil D, Barak S, Khatkar BS (2014). J Food Sci Technol 51: 409–418
14. Yamamoto Y (2001). J Japan Soc Nutr Food Sci 54:139–145
15. Zhang LM, Zhou JF, Hui PS (2005). J Sci Food Agric 85:2638–2644
16. Hasan AMA, Abdel-Raouf ME (2018). Egypt J Pet 27:1043–1050
17. Jano A, Lame A, Kokalari E (2012). Kemija u industriji (J Chem Chem Eng) 61(11–12):497–503
18. About S, Zouarhi M, Chebabe D, Damej M, Berisha A, Hajjaji N (2020). Heliyon 6(3):e03574
19. Mothé CG, Correia DZ, de França FP, Riga AT (2006). J Therm Anal Calorim 85:31–36
20. Adewole JK, Muritala KB (2019). J Petrol Explor Prod Technol 9(3):2297–2307
21. Mohayeji M, Farsi M, Rahimpour MR, Shariati A (2016). J Taiwan Inst Chem Eng 60:76–82
22. Caputo HE, Strau JE, Grinstaff MW (2019). Chem Soc Rev 48: 2338–2365
23. Wang X, Wang J, Zhang J, Zhao B, Yao J, Wang Y (2009). Int J Biol Macromol 46(1):59–66
24. Mestechkina NM, Egorov AV, Shcherbukhin VD (2006). Appl Biochem Microbiol 4:326
25. Wang J, Zhao B, Wang X, Yao J, Zhang J (2012). Int J Biol Macromol 50(5):1201–1206
26. Al-Horani RA, Desai UR (2010). Tetrahedron 66(16):2907–2918
27. Kazachenko AS, NYu V, Sudakova IG, Levdansky VA, Lutoshkin MA, Kuznetsov BN (2020). J Sib Fed Univ Chem 13(2):232–246
28. Pen RZ (2014) Planning an experiment at Statgraphics Centurion. Krasnoyarsk: SibSTU 293
29. Becke AD (1988). Phys Rev A 38:3098–3100
30. Perdew JP, Burke K, Wang Y (1996). Phys Rev B 54:16533–16539
31. Young D (2001) Computational chemistry: a practical guide for applying techniques to real world problems, vol 408. Wiley, New York
32. Frisch MJ, Trucks GW, Schlegel HB, Scuseria GE, Robb MA, Cheeseman JR, Scalmani G, Barone V, Mennucci B, Petersson GA, et al (2010) Gaussian, Inc., Wallingford
33. Dennington R, Keith T, Millam J (2010) Gauss View, Version 5. Semichem Inc., Shawnee Mission
34. Parr RG, Pearson RG (1983). J Am Chem Soc 105:7512–7516
35. Noureddine O, Gatfaoui S, Brandan SA, Marouani H, Issaoui N (2020). J Mol Struct 1202:127351
36. Gatfaoui S, Issaoui N, Roisnel T, Marouani H (2019). J Mol Struct 1191:183–196
37. Mudgil D, Barak S, Khatkar BS (2012). J Biol Macromol 50(4): 1035–1039
38. Wang Q, Ellisa PR, Ross-Murphy SB (2003). Carbohyd Polym 53: 75–83
39. Sagaama A, Noureddine O, Brandan SA, Jedryka AJ, Flakus HT, Ghalla H, Issaoui N (2020). Comput Biol Chem 87:107311
40. Issa TB, Sagaama A, Issaoui N (2020). Comput Biol Chem 86: 107268
41. Gatfaoui S, Sagaama A, Issaoui N, Roisnel T, Marouani H (2020). Solid State Sci:106326
42. Noureddine O, Gatfaoui S, Brandan SA, Sagaama A, Marouani H, Issaoui N (2020). J Mol Struct 1207:127762
43. Jomaa I, Noureddine O, Gatfaoui S, Issaoui N, Roisnel T, Marouani H (2020). J Mol Struct 1213:128186
44. Noureddine O, Gatfaoui S, Brandán SA, Marouani H, Issaoui N (2020). J Mol Struct 1202:127351
45. Politzer P, Murray JS (2018). J Comput Chem 39:464–471
46. Politzer P, Murray JS (2020). ChemPhysChem 21:579–588
47. Politzer P, Murray JS, Clark T (2015). Top Curr Chem 358:19–42